Simulations of RMP Configurations for Tungsten Impurity control in EAST Tokamak

Z.H. Gao[1], S.Y. Dai[1,*], Z.X. Wen[1], H.M. Zhang[2], G.Z. Hao[3], Y. Feng[4], D.Z. Wang[1]

[1]Key Laboratory of Materials Modification by Laser, Ion and Electron Beams (Ministry of Education), School of Physics, Dalian University of Technology, Dalian, China
[2]Hefei Institutes of Physical Science, Chinese Academy of Sciences, Hefei, China
[3]Southwestern Institute of Physics, Chengdu, China
[4]Max-Planck-Institute für Plasmaphysik, Greifswald, Germany
*Corresponding author. Email: daishuyu@dlut.edu.cn

ABSTRACT

High-Z tungsten (W) accumulation in EAST degrades plasma performance and threatens steady-state operation. Optimization of resonant magnetic perturbation (RMP) phasing is investigated to mitigate W sputtering and accumulation, using MARS-F coupled with EMC3-EIRENE impurity-transport simulations. The impurity-suppression phase inferred from vacuum fields peaks at $\Delta\phi = 0^\circ$, whereas inclusion of plasma response shifts the effective phase to $\Delta\phi = 90^\circ$ owing to screening and amplification. Complete W-suppression windows appear only with plasma response for n = 1, spanning $\Delta\phi \approx 0^\circ - 135^\circ$. The mechanism is resonant amplification of edge perturbations that enhances boundary stochasticity, increases recycling, and lowers target temperatures, reducing incident ion energy below W sputtering thresholds. The $\Delta\phi$ range that suppresses edge-localized modes in EAST overlaps with the window for W reduction, suggesting that established ELM-suppression criteria based on the total field at the last rational surface can serve as proxies for impurity control efficacy. These findings provide actionable guidance for RMP phasing to minimize tungsten sources and accumulation on EAST.

OBJECTIVES

- **RMP Phasing Optimization:** To investigate the impact of upper/lower coil phase difference on tungsten impurity sputtering, transport, and radiation, aiming to identify the optimal RMP phase configuration for impurity mitigation.
- **Plasma Response Assessment:** To evaluate the role of plasma response fields, obtained from MARS-F calculations, in modifying edge magnetic topology and influencing impurity behavior compared with vacuum field cases.

MODELS

- **Plasma Response Model (MARS-F)**
  - **Purpose:** Compute vacuum and plasma-response magnetic perturbations generated by RMP coils.
  - **Physics Basis:** Linear single-fluid MHD equations solved in full toroidal geometry using the equilibrium from CHEASE code as input.
  - **Outputs:** 3D perturbed magnetic field δB.
  - **Key Parameters:** Upper/lower coil phase difference ($\Delta\phi$), Coil current amplitude (I), toroidal mode number (n) and equilibrium profile.
- **Edge Plasma & Impurity Transport Model (EMC3-EIRENE)**
  - **Purpose:** Simulate 3D plasma transport and tungsten impurity behavior under RMP fields.
  - **Physics Framework:**
    - **EMC3:** Solves multi-fluid plasma transport (continuity, momentum, and energy) along distorted 3D magnetic field lines.
    - **EIRENE:** Solves neutral transport and recycling using Monte Carlo methods.
  - **Key Features:** Tungsten sputtering sources determined by local ion flux and incident energy (Eckstein model) and following transport process under RMP fields.

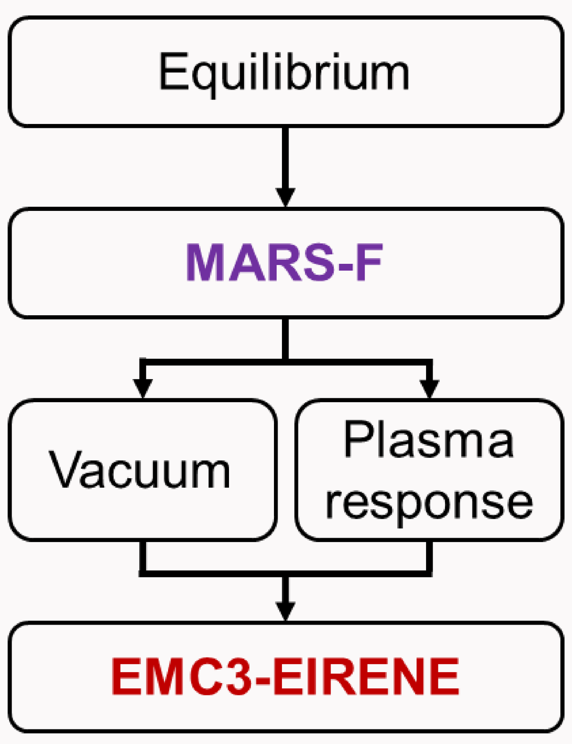

- **Key Input Parameters:**

Toroidal mode number: n = 1
Coil current amplitude: $I = 8.8kAt$
Input power: $P_{SOL} = 2.3MW$
Upstream density: $n_u = 2.1 \times 10^{19} m^{-3}$
Particle perpendicular transport coefficient: $D_\perp = 0.15 m^2 s^{-1}$
Energy perpendicular transport coefficient: $\chi_\perp = 0.8\, m^2 s^{-1}$
Impurity perpendicular transport coefficient: $D_{imp} = 1.5\, m^2 s^{-1}$

RESULTS

1. Plasma response versus coil phasing

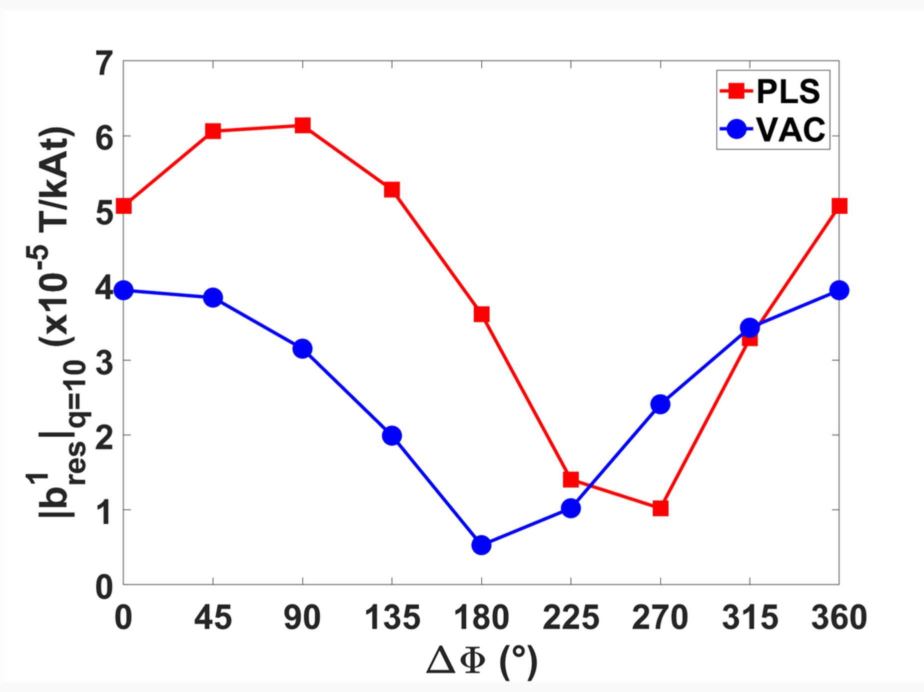

Phase scan of the resonant normal field amplitude $|b^1_{res}|$ at the q = 10 rational surface as a function of the coil phase difference $\Delta\phi$ for n = 1 RMPs, from MARS-F calculations.

- Across most phases the PLS amplitude exceeds the VAC value.
- The VAC minimum appears near $\Delta\phi \approx 180^\circ$, while the PLS minimum is shifted to $\Delta\phi \approx 270^\circ$.

2. Effect on target erosion

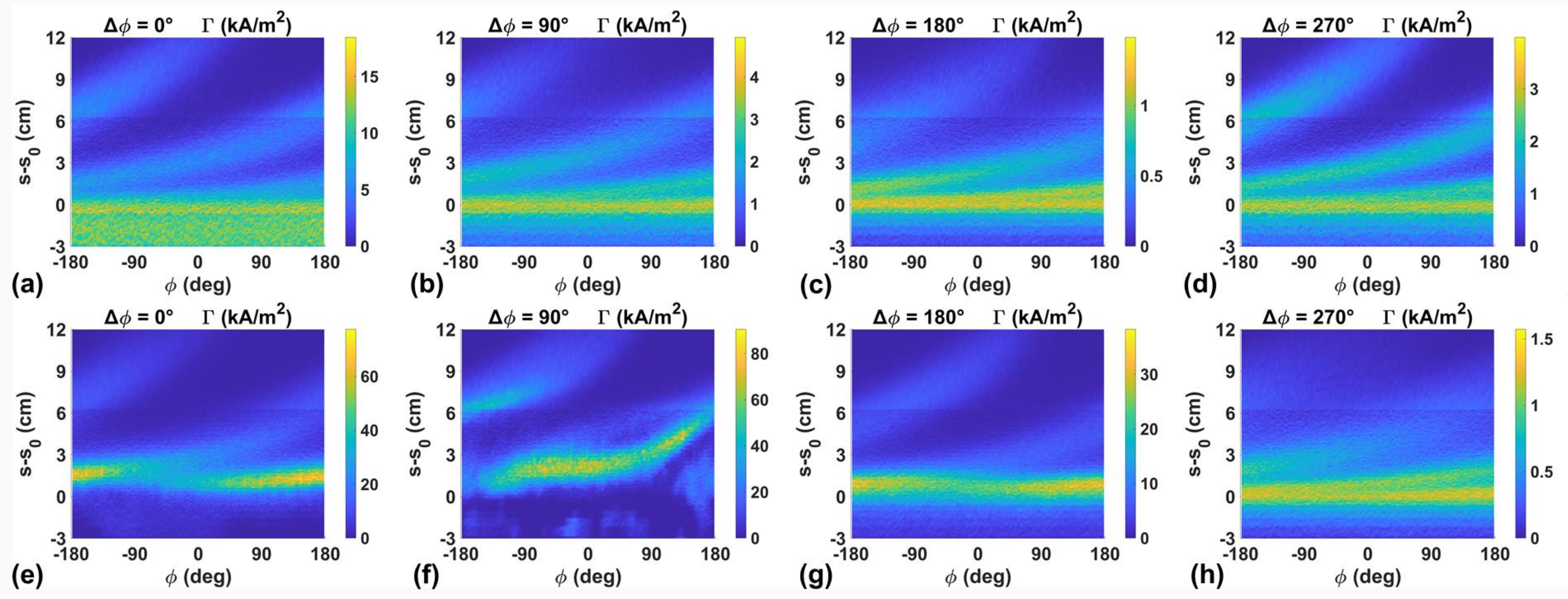

2D distributions of particle flux for vacuum (upper panel) and plasma response (lower panel) fields in different coil phase difference ($\Delta\phi$) near the outer upper target.

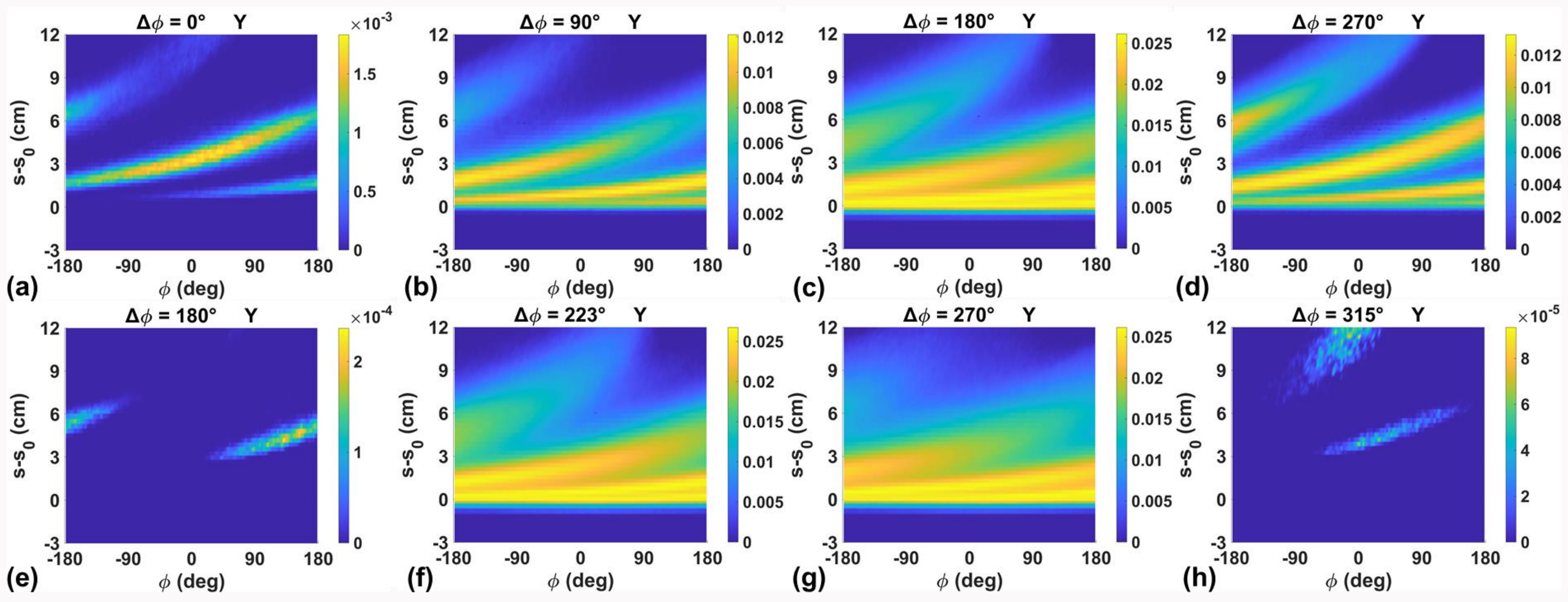

2D distributions of sputtering yield for vacuum (upper panel) and plasma response (lower panel) fields in different coil phase difference ($\Delta\phi$) near the outer upper target.

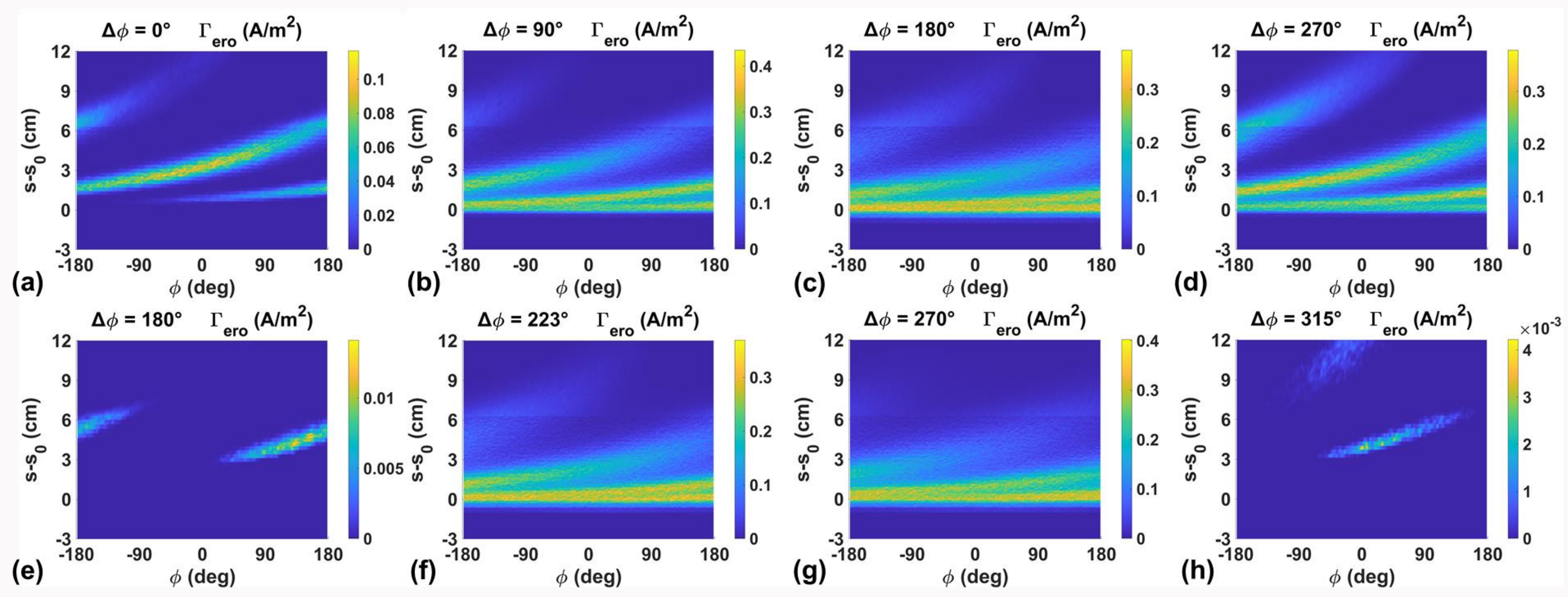

2D distributions of W erosion flux for vacuum (upper panel) and plasma response (lower panel) fields in different coil phase difference ($\Delta\phi$) near the outer upper target.

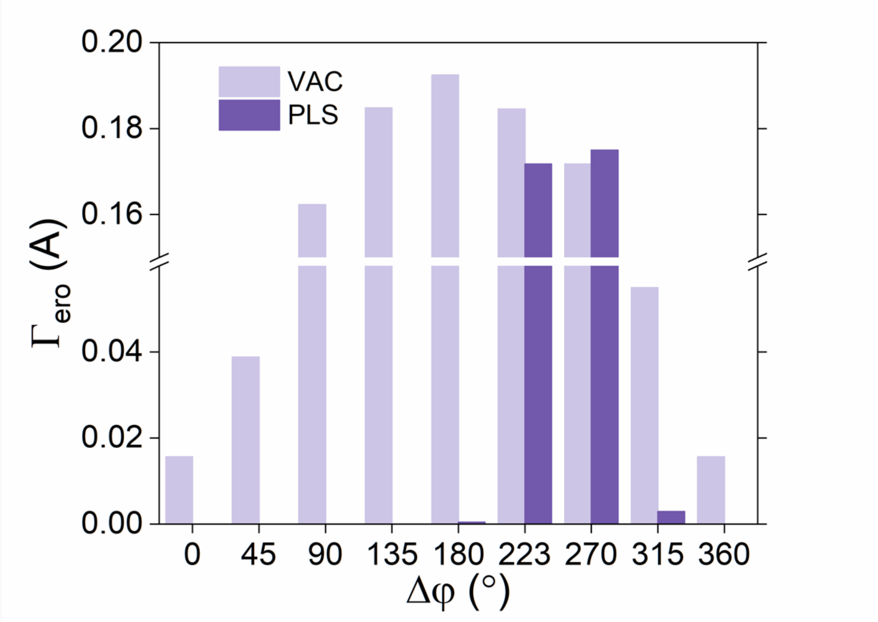

- As the perturbation increases, the higher temperature enhances erosion at the second strike point, while it vanishes at the first.
- The phase selectivity and overall reduction of Γ_{ero} are consistent with RMP-induced modifications of edge magnetic topology.
- The VAC minimum appears near $\Delta\phi \approx 0^\circ$, while the PLS is completely inhibited within 0 - 180°.

3. Effect on impurity amount

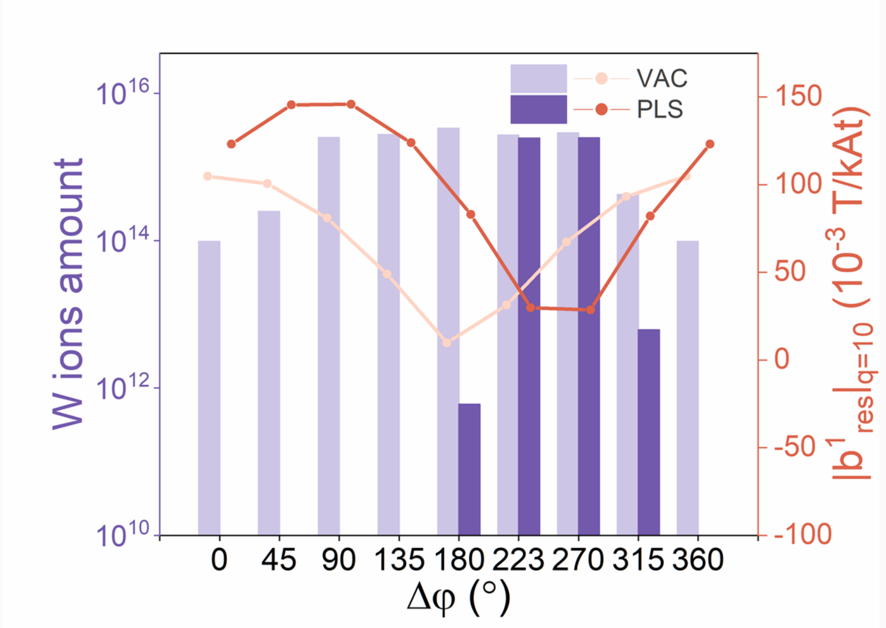

Phase dependence of tungsten ion inventory (bars, left log axis) and resonant normal field $|b^1_{res}|$ at q = 10 (right axis) versus upper/lower coil phase difference $\Delta\phi$.

- An extended impurity-suppression window appears for $\Delta\phi \lesssim 180^\circ$ for PLS cases, during which the W inventory is reduced by orders of magnitude relative to the VAC case.

SUMMARY

- Coupled MARS-F and EMC3–EIRENE simulations reveal that including plasma response amplifies the resonant edge field and shifts its phase by ~90° relative to the vacuum case.
- A clear impurity-suppression window ($\Delta\varphi \approx 0^\circ$–$135^\circ$, extending toward ~180°) emerges only with plasma response, during which W erosion and edge inventory drop by orders of magnitude. The mitigation mechanism arises from enhanced edge stochasticity and cooler targets, reducing ion impact energy below the W sputtering threshold.
- The W-suppression window aligns closely with the ELM-suppression window, revealing a shared operational regime where both tungsten mitigation and ELM control are simultaneously optimized.